



Physical and Electrochemical Properties of Soluble 3,4-Ethylenedioxythiophene (EDOT)-Based Copolymers Synthesized *via* Direct (Hetero) Arylation Polymerization

Qiang Guo¹, Jincheng Zhang¹, Xiaoyu Li², Heqi Gong¹, Shuanghong Wu³ and Jie Li^{1*}

¹College of Optoelectronic Engineering, Chengdu University of Information Technology, Chengdu, China, ²Southwest University of Science and Technology, Mianyang, China, ³School of Optoelectronic Science and Engineering, University of Electronic Science and Technology of China, Chengdu, China

OPEN ACCESS

Edited by:

Mina Mazzeo,
University of Salerno, Italy

Reviewed by:

Isao Yamaguchi,
Shimane University, Japan
Fatma Baycan,
Çanakkale Onsekiz Mart University,
Turkey
Shiming Zhang,
Nanjing Tech University, China
Asit Patra,
National Physical Laboratory (CSIR),
India

*Correspondence:

Jie Li
lijie@cuit.edu.cn

Specialty section:

This article was submitted to
Polymer Chemistry,
a section of the journal
Frontiers in Chemistry

Received: 05 August 2021

Accepted: 20 September 2021

Published: 29 October 2021

Citation:

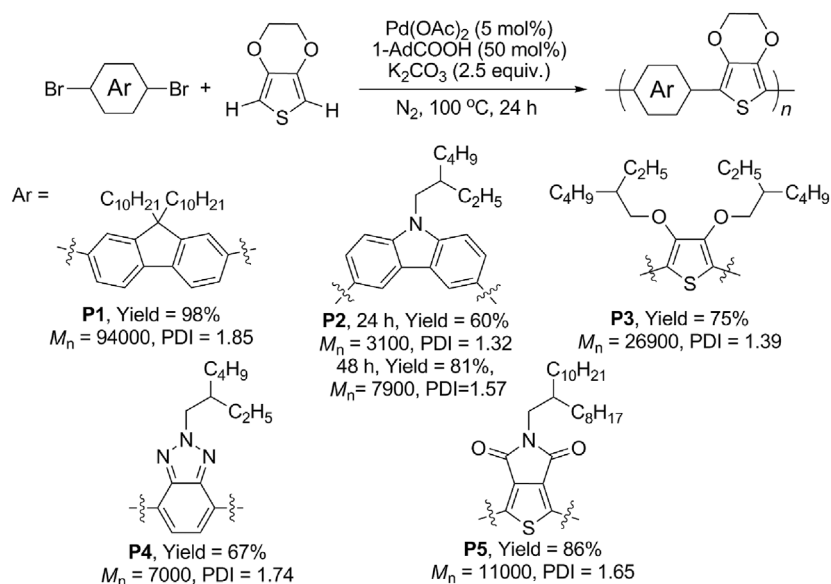
Guo Q, Zhang J, Li X, Gong H, Wu S
and Li J (2021) Physical and
Electrochemical Properties of Soluble
3,4-Ethylenedioxythiophene (EDOT)-
Based Copolymers Synthesized *via*
Direct (Hetero)
Arylation Polymerization.
Front. Chem. 9:753840.
doi: 10.3389/fchem.2021.753840

Over the past decades, π -conjugated polymers (CPs) have drawn more and more attention and been essential materials for applications in various organic electronic devices. Thereinto, conjugated polymers based on the 3,4-ethylenedioxythiophene (EDOT) backbone are among the high-performance materials. In order to investigate the structure–property relationships of EDOT-based polymers and further improve their electrochemical properties, a series of organic solvent–soluble EDOT-based alternative copolymers consisting of electron-rich fragments (fluorene **P1**, carbazole **P2**, and 3,4-alkoxythiophene **P3**) or electron-deficient moieties (benzotriazole **P4** and thieno[3,4-*c*]pyrrole-4,6-dione **P5**) were synthesized *via* direct C–H (hetero)arylation polymerization (DHAP) in moderate to excellent yields (60–98%) with medium to high molecular weights ($M_n = 3,100$ –94,000 Da). Owing to their various electronic and structural properties, different absorption spectra ($\lambda_{max} = 476, 380, 558, 563, \text{ and } 603 \text{ nm}$) as well as different specific capacitances of 70, 68, 75, 51, and 25 F/g with 19, 10, 21, 26, and 69% of capacity retention after 1,000 cycles were observed for **P1–P5**, respectively. After careful study through multiple experimental measurements and theoretical calculation, appropriate electronic characteristics, small molecular conformation differences between different oxidative states, and well-ordered molecular stacking could improve the electrochemical performance of CPs.

Keywords: direct hetero(arylation) polymerization, conjugated copolymer, electrochemical, structure–property relationship, 3,4-ethylenedioxythiophene (EDOT)

INTRODUCTION

With the rapid development in the field of wearable and flexible electronics during the past decades, π -conjugated polymers (CPs) have drawn more and more attention and been essential materials for applications in organic solar cells (OSCs) (Dou et al., 2013), organic field-effect transistors (OFETs) (Olivier et al., 2014), electrochromic devices (ECDs) (Jensen et al., 2015), and electrochemical



SCHEME 1 | Direct hetero(arylation) polymerization of various EDOT-based CPs.

capacitors (ECs) (Han and Dai, 2019) because of CPs' excellent electronic, optoelectronic, and mechanical properties. Thereinto, CP-based ECs are considered one of the next-generation alternative energy storage systems, featuring a number of advantages including low cost, lightweight, environmental friendliness, flexibility, fast charge/discharge capability, and relatively high charge storage capacity. Meanwhile, it is widely accepted that the electrode material plays a crucial role in the capacitive performance of a supercapacitor, and lots of efforts have been put toward the development of new and high-performance electrode materials (Meng et al., 2017). Among all kinds of CPs, polyaniline (PANI), polypyrrole (PPy), and polythiophene (PTh) derivatives have been widely investigated as the active electrode materials in ECs with high pseudocapacitance and low cost. It has been reported that conjugated polymers based on the 3,4-ethylenedioxythiophene (EDOT) backbone exhibit excellent redox activity, high conductivity, and fast redox switching speeds (Liu and Reynolds, 2010). In order to further improve their electrochemical properties, nano-structuring, composite, blending, and copolymerization approaches based on EDOT were attempted and performed well (Shown et al., 2015). Particularly, copolymerization would be a valuable and potential method because the resultant new copolymer would combine the positive properties of both monomers. To date, EDOT-based electrode materials were typically fabricated *via* electropolymerization or *in situ* oxidative chemical polymerization on the current collectors. Accordingly, the molecular structure types of polymers synthesized by these two methods are relatively limited, which is not conducive to the study of the structure–property relationship. For example, the A–B alternative copolymer cannot be readily synthesized by classical electropolymerization or oxidative chemical polymerization. Moreover, the products of

electropolymerization generally have problems in further processing, large-scale preparation, and limited molecular structure diversity, due to their infusibility and poor solubility in common solvents. And the products of oxidative chemical polymerization also have problems in the metal ion residue and low reactivity for electron-deficient monomers. In other words, to design more appropriate synthetic methods is of crucial importance to the development of high-performance CPs.

Over the past decade, transition metal-catalyzed direct C–H (hetero)arylation polymerization (DHAP) of non-preactivated (hetero)arenes with (hetero)aryl halides is one of the most ideal and effective methods to construct conjugated polymers, avoiding tedious reaction steps and formation of stoichiometric toxic organometallic byproducts in the traditional organometallic couplings (Mercier and Leclerc, 2013). Furthermore, as compared to electropolymerization and oxidative chemical polymerization methods, π -conjugated polymers synthesized *via* DHAP have been widely applied in the field of high-performance organic semiconductors and have shown a variety of merits, such as a well-defined structure, a diversified molecular structure, high reproducibility, large-scale throughput, and good solubility (Wu et al., 2017). Based on the broad applicability and our continuous efforts in constructing CPs *via* DHAP (Guo et al., 2013; Guo et al., 2016), we herein present a new work in that five organic solvent-soluble EDOT-based alternative copolymers consisting of electron-rich fragments (fluorene, carbazole, and 3,4-alkoxythiophene) or electron-deficient moieties (benzotriazole and thieno[3,4-*c*]pyrrole-4,6-dione) were synthesized effectively *via* DHAP in moderate to excellent yields (60–98%) with medium to high molecular weights ($M_n = 3,100$ –94,000 Da). Although several similar examples of these polymers have been synthesized before, the relationships between the photophysical and electrochemical properties and

TABLE 1 | Physical, electrochemical, and conformational properties of **P1–P5**.

Polymer	Experimental data							Calculated data ^h	
	$\lambda_{\text{solution}}$ [nm] ^a	λ_{film} [nm] ^b	C [F/g] ^c	C _{retention} ^d (%)	IR _{drop} [V] ^e	R _a [nm] ^f	T _d [°C] ^g	θ_{dihedral} [°] ⁱ	RMSD ^j
P1	471	476	70	19	0.25	3.91	389	27.15	0.6324
P2	359	380	68	10	0.25	4.08	371	29.57	0.6485
P3	547	558	75	21	0.08	3.10	316	2.88	0.5437
P4	546	563	51	26	0.09	2.91	354	10.81	0.3827
P5	580	603	25	69	0.09	2.08	394	2.19	0.1129

^aMaximum absorption wavelength in dilute CH₂Cl₂ solution.

^bMaximum absorption wavelength in the film deposited by spray coating on a quartz plate.

^cSpecific capacitance at a scan rate of 100 mV s⁻¹.

^dCapacity retention after 1,000 cycles at a scan rate of 100 mV s⁻¹.

^eIR_{drop} values measured during the discharge process at 10 A g⁻¹.

^fSurface average roughness determined by AFM.

^gTemperature at 5% weight loss under nitrogen.

^hBased on the optimized dimers.

ⁱDihedral angles between two units.

^jMaximum value of RMSD between neutral, 50% doped, and 100% doped states.

their structures have not been systematically investigated (Yamazaki et al., 2013; Kuwabara et al., 2014; Kerszulis et al., 2015; Li et al., 2016a; Robitaille et al., 2017). The relationships between CPs' molecular structures and their electrochemical properties and microscopic packing properties were carefully investigated through cyclic voltammetry (CV), galvanostatic charge–discharge (GCD), atomic force microscopy (AFM), X-ray diffraction (XRD) analysis, and density functional theory (DFT) calculation. The results indicated that all the physical and electrochemical properties of these EDOT-based CPs were predominantly determined by their electronic characteristics, molecular planarity, and rigidity.

RESULTS AND DISCUSSION

Owing to the wide application of EDOT-based CPs and high reactivity of C–H bonds, the DHAP of EDOT was early and extensively studied by several research groups (Yamazaki et al., 2013; Elsayy et al., 2015; Hayashi and Koizumi, 2015; Li and Michinobu, 2016). Based on these works, a catalytic system combining Pd(OAc)₂ (5 mol%), K₂CO₃ (2.5 equiv.), and 1-adamantanecarboxylic acid (1-AdCOOH, 50 mol%) in DMAc at 100 °C for 24 h was used to synthesize our EDOT-based CPs. As shown in **Scheme 1**, both electron-rich units (fluorene **P1**, carbazole **P2**, and 3,4-alkoxythiophene **P3**) and electron-deficient units (benzotriazole **P4** and thieno[3,4-*c*]pyrrole-4,6-dione **P5**) were successfully engaged in the reactions, offering structure-diversified EDOT-based CPs in moderate to excellent yields (60–98%) with medium to high molecular weights (M_n = 3,100–94,000 Da). The yield and molecular weight of **P2** can be further improved up to 81% and 7,900 Da after 48 h, respectively, indicating its relatively low reactivity of 3,6-dibromocarbazole. The good yields of **P1–P5** with comparable or even higher M_n compared to those obtained in previous works indicated the high reactivity of EDOT under this catalytic system and good applicability of DHAP (Yamazaki et al., 2013; Kerszulis et al.,

2015; Li et al., 2016a). It is obvious that the yields and molecular weights of these polymers were closely related to the numbers and lengths of alkyl chains attached on the backbone, namely, good solubility of products can improve the yields and molecular weights. And the relatively low molecular weight of **P4** was probably attributed to its limited solubility because a small amount of insoluble polymer remained in the cartridge after extraction with chloroform. All the polymer structures were confirmed by ¹H NMR and MALDI-TOF mass spectrometry. The ¹H NMR spectra of **P1**, **P2**, and **P3** were in agreement with those in the literature (Yamazaki et al., 2013; Kerszulis et al., 2015; Li et al., 2016a). Br terminals can be found in the MALDI-TOF mass spectrum, suggesting the DHAP can be further carried out to provide high-molecular-weight products. Owing to the solubility of **P1–P5** in common solvents (CH₂Cl₂, CHCl₃, and THF), films for characterization of UV-Vis absorption, electrochemical properties, and microscopic packing properties were fabricated by solution processing, such as drip coating and spray coating.

The UV-Vis spectra and data of these five EDOT-based CPs in diluted solution and in films are shown in **Supplementary Figure S1** and summarized in **Table 1**, respectively. Moreover, to gain insight into the structure–photophysical property relationship, the geometries of two repeating unit molecular models for polymers **P1–P5** were optimized through density functional theory (DFT), as shown in **Supplementary Figures S15–S19**. And the dihedral angles between two units (**Table 1**) were calculated to measure the coplanarity of polymer molecules. The remarkably different absorption spectra of **P1–P5**, covering the near-UV and blue, green, and red color regions, suggest their distinct electronic and structural properties. The obviously red-shifted absorption of **P1–P5** in the thin film in comparison with that in the solution could be generated from the strong intermolecular interaction between the polymer backbones in film states. On comparison with **P1** and **P2** containing electron-rich units ($\lambda_{\text{solution}}$ = 471, 359 nm and λ_{film} = 476, 380 nm, respectively), **P4** and **P5** with electron-deficient

units displayed significantly red-shifted absorption ($\lambda_{\text{solution}} = 546, 580 \text{ nm}$ and $\lambda_{\text{film}} = 563, 603 \text{ nm}$, respectively), which should be assigned to the intramolecular charge transfer (ICT) from the EDOT donor to corresponding electron-deficient acceptor units. When connecting 3,4-alkoxythiophene with EDOT, **P3** also displayed a red-shifted absorption ($\lambda_{\text{solution}} = 547 \text{ nm}$ and $\lambda_{\text{film}} = 558 \text{ nm}$), owing to its almost planar backbone ($\theta_{\text{dihedral}} = 2.88^\circ$) induced by an intramolecular O...S interaction (Gleiter et al., 2018). Thus, combining the ICT property and good coplanarity (2.19°), **P5** exhibited the most red-shifted maximum absorption wavelength among these five polymers, implying its efficient electron delocalization, transport property, and close molecular stacking.

Electrochemical measurements were performed in a three-electrode cell with a platinum wire as the counter electrode, an Ag/Ag⁺ wire (silver wire in 0.01 M AgNO₃ in acetonitrile) as the reference electrode, and a Pt disk or foam-nickel electrode drop-coated with the polymer as the working electrode and using 0.1 M tetrabutylammonium hexafluorophosphate in dry acetonitrile as the electrolyte solution. Firstly, cyclic voltammetry (CV) measurements of **P1–P5** films on a Pt disk electrode were performed to analyze their p-doping/dedoping processes at a scan rate of 100 mV s⁻¹ (Supplementary Figure S2). The different CV curves indicated large differences in their electrochemical properties. The corresponding HOMO energy levels were then estimated according to the following equation: HOMO = $-(4.80 + E_{\text{ox,onset}})$ eV, where $E_{\text{ox,onset}}$ is the onset potential of the oxidation peak with respect to the ferrocene/ferrocenium (Fc/Fc⁺) redox couple. The HOMO energy levels of **P1** (-5.17 eV), **P2** (-5.06 eV), and **P3** (-4.79 eV) are in good agreement with those reported by other groups (-5.2 eV , -5.09 eV , and $\sim -4.8 \text{ eV}$, respectively) (Kuwabara et al., 2014; Kerszulis et al., 2015; Li et al., 2016a). Compared to the lowest HOMO energy level of **P5** (-5.35 eV) among **P1–P5**, the coplanar and electron-rich **P3** showed the highest HOMO energy level (-4.79 eV), indicating its easiness of losing electrons and the potential development of new polymeric anodes. The arrangement trends of HOMO energy levels of **P1–P5** estimated by CV were in accordance with those of HOMO values calculated by DFT, besides slightly overestimated HOMO and LUMO levels by DFT (Supplementary Table S1 and Supplementary Figure S20). Subsequently, the electrochemical properties of **P1–P5** on a foam-nickel electrode were further examined and investigated through CV at different scan rates, galvanostatic charge–discharge (GCD) curves, and electrochemical impedance spectroscopy (EIS) and are summarized in Table 1 and Supplementary Figures S3–S7. The kept shapes of current density–potential profiles at gradually increasing scan rates from 5, 10, 20, 50, 100, to 200 mV s⁻¹ demonstrated their fast redox behaviors and high rate charge/discharge performances (Yigit and Gullu, 2018). For these polymers, their oxidation peak current densities were nearly linear with the corresponding scan rates (Supplementary Figure S8), suggesting that all polymers immobilized on the electrode surfaces very well and the redox processes are non-diffusional-controlled (Li et al., 2016b). From the shapes of CV and GCD curves (Supplementary Figures S3–S7), it can be seen that all

polymers **P1–P5** exhibited obvious pseudocapacitive energy storage properties. The measured specific capacitances of the polymers (**P1–P5**)/foam-nickel electrode were calculated to be 70, 68, 75, 51, and 25 F/g (at 100 mV s⁻¹) with 19, 10, 21, 26, and 69% of capacity retention after 1,000 cycles, respectively. These specific capacitances were higher than those of some other conducting polymer electrodes deposited by solution processing methods (Sun et al., 2020a; Sun et al., 2020b), probably owing to the excellent redox activity of EDOT. Together with the analysis of molecular structures, these data illustrate that the introduction of electron-donating units into the polymer backbone can improve the charge storage capacity, and the different cycle stabilities might be due to their different structure properties and/or microstructures. The GCD curves of **P1–P5** at various constant current densities exhibited deviation from the triangular geometry with a linear charge/discharge process and slight distortion, suggesting the existence of electrochemical double-layer behaviors, besides pseudocapacitive contribution by CPs. In contrast, the IR_{drop} values of **P3–P5** were much smaller than those of **P1–P2**, implying a small internal resistance which was probably attributed to their less twisted conformation. The Nyquist plots of all polymers exhibited a straight line in the low-frequency range with a negligible semicircle in the high-frequency range (Supplementary Figure S9), indicating the fast charge transfer between the electrode and the electrolyte surface (Zhang et al., 2016).

It is known that the electrochemical properties are closely related to the surface features and internal stacking characteristics (Fong et al., 2017). Thus, AFM and XRD characterization were performed to measure the surface morphologies and molecular packing patterns of these redox polymers, respectively. As demonstrated by AFM and shown in Supplementary Figures S10–S12, all the films of **P1–P5** exhibited continuous and uniform morphologies, indicating homogeneous films obtained by solution processing methods, which is beneficial to the improvement of charge transfer. From the distinct XRD patterns of **P5** (Supplementary Figure S13), diffraction peaks were observed at $2\theta = 3.43, 6.79, 9.94, \text{ and } 25.54^\circ$, corresponding to d -spacings of 25.73, 13.01, 8.89, and 3.48 Å, respectively, representing the existence of lamellar stacking and π – π stacking of polymer main chains. With the lowest roughness and best XRD crystallinity of **P5** among all polymers, the relatively good cyclic stability could be attributed to the homogeneous surface and well-ordered stacking of molecules in films. All the thermal degradation temperatures (T_d) over 300°C of **P1–P5** at 5% weight loss manifested their good thermal stability (Supplementary Figure S14), which is conducive to further annealing processing and device applications.

To further investigate the influence of molecular structures on their cyclic stability, geometry optimizations of two repeating units at neutral, 50% doped, and 100% doped states were carried out by DFT calculations (see the Supplementary Material for details) (Murto et al., 2020). The geometry changes between neutral, 50% doped, and 100% doped states are measured by the root-mean-squared displacement (RMSD), and the maximum RMSD values are summarized in Table 1.

Obviously, the minimum RMSD (0.1129) of **P5** implied the least backbone distortions at different oxidative states, which is favorable to electrochemical stability during the charge/discharge cycles and is responsible for the good cycling stability of **P5** compared to those of the others. It is interesting that the thiophene backbone of **P3** featured coplanar conformations besides obvious rotations of methoxy groups at neutral, 50% doped, and 100% doped states, thus causing a large RMSD of 0.5437. The increased RMSD means large volumetric changes induced by swelling and shrinkage during the charge/discharge process, which might be the reason for the greatly improved cycling stability when the alkoxy groups attached to thiophene were fixed by forming a seven-membered ring (Osterholm et al., 2016).

CONCLUSION

In this work, a series of novel soluble EDOT-based conjugated copolymers consisting of electron-rich or electron-deficient units were synthesized steadily in moderate to excellent yields (60–98%) with medium to high molecular weights ($M_n = 3,100\text{--}94,000$ Da) through direct (hetero)arylation polymerization. Owing to the structural diversity of obtained EDOT-based copolymers, the varied absorption spectra, specific capacitance, and capacity retention were observed, which should be attributed to the electronic characteristics of various units introduced, molecular torsions in the polymer backbone, and thus resultant different surface morphologies and molecular packings. Clear redshifts in absorption of **P3**, **P4**, and **P5** were observed, due to their good coplanarity and/or ICT property. When using a foam-nickel electrode drop-coated with the polymer as the working electrode in a three-electrode cell, good specific capacitances of 70, 68, 75, 51, and 25 F/g (at 100 mV s^{-1}) with 19, 10, 21, 26, and 69% of capacity retention after 1,000 cycles for **P1–P5** were obtained, respectively, owing to the good redox activity of the EDOT unit. The results of our present study confirm that appropriate electronic characteristics, fast charge transfer, good coplanarity, low RMSD between

different oxidative states, homogeneous surface, and well-ordered molecular stacking could improve the cycling stability of polymeric capacitive performance which is still one of the main obstacles in further applications of supercapacitors based on π -conjugated polymers. It is anticipated that such study will provide a novel strategy for the molecular design of π -conjugated polymers regarding electrochemical properties.

DATA AVAILABILITY STATEMENT

The original contributions presented in the study are included in the article/**Supplementary Material**, and further inquiries can be directed to the corresponding author.

AUTHOR CONTRIBUTIONS

QG and JL conceived the research and supervised the whole work. JZ, XL, and HG prepared materials and characterized the physical and electrochemical properties. QG, XL and SW contributed to theoretical calculations. All authors contributed to manuscript revision and approved the submitted version.

FUNDING

This work was financially supported by the National Natural Science Foundation of China (Grant Nos. 21801028, 61505015) and Department of Science and Technology of Sichuan Province (Grant Nos. 2019YJ0358, 2020YFG0038, 2017FZ0085).

SUPPLEMENTARY MATERIAL

The Supplementary Material for this article can be found online at: <https://www.frontiersin.org/articles/10.3389/fchem.2021.753840/full#supplementary-material>

REFERENCES

- Dou, L., You, J., Hong, Z., Xu, Z., Li, G., Street, R. A., et al. (2013). 25th Anniversary Article: A Decade of Organic/polymeric Photovoltaic Research. *Adv. Mater.* 25, 6642–6671. doi:10.1002/adma.201302563
- Elsawy, W., Son, M., Jang, J., Kim, M. J., Ji, Y., Kim, T.-W., et al. (2015). Isoindigo-Based Donor-Acceptor Conjugated Polymers for Air-Stable Nonvolatile Memory Devices. *ACS Macro Lett.* 4, 322–326. doi:10.1021/mz500698p
- Fong, K. D., Wang, T., and Smoukov, S. K. (2017). Multidimensional Performance Optimization of Conducting Polymer-Based Supercapacitor Electrodes. *Sustainable Energ. Fuels* 1, 1857–1874. doi:10.1039/c7se00339k
- Gleiter, R., Haberhauer, G., Werz, D. B., Rominger, F., and Bleiholder, C. (2018). From Noncovalent Chalcogen-Chalcogen Interactions to Supramolecular Aggregates: Experiments and Calculations. *Chem. Rev.* 118, 2010–2041. doi:10.1021/acs.chemrev.7b00449
- Guo, Q., Dong, J., Wan, D., Wu, D., and You, J. (2013). Modular Establishment of a Diketopyrrolopyrrole-Based Polymer Library via Pd-Catalyzed Direct C-H (Hetero)arylation: A Highly Efficient Approach to Discover Low-Bandgap Polymers. *Macromol. Rapid Commun.* 34, 522–527. doi:10.1002/marc.201200737
- Guo, Q., Wu, D., and You, J. (2016). Oxidative Direct Arylation Polymerization Using Oxygen as the Sole Oxidant: Facile, green Access to Bithiazole-Based Polymers. *ChemSusChem* 9, 2765–2768. doi:10.1002/cssc.201600827
- Han, Y., and Dai, L. (2019). Conducting Polymers for Flexible Supercapacitors. *Macromol. Chem. Phys.* 220, 1800355. doi:10.1002/Macp.201800355
- Hayashi, S., and Koizumi, T. (2015). Chloride-promoted Pd-Catalyzed Direct C-H Arylation for Highly Efficient Phosphine-free Synthesis of π -conjugated Polymers. *Polym. Chem.* 6, 5036–5039. doi:10.1039/c5py00871a
- Jensen, J., Hösel, M., Dyer, A. L., and Krebs, F. C. (2015). Development and Manufacture of Polymer-Based Electrochromic Devices. *Adv. Funct. Mater.* 25, 2073–2090. doi:10.1002/adfm.201403765
- Kerszulis, J. A., Johnson, K. E., Kuepfert, M., Khoshabo, D., Dyer, A. L., and Reynolds, J. R. (2015). Tuning the painter's Palette: Subtle Steric Effects on Spectra and Colour in Conjugated Electrochromic Polymers. *J. Mater. Chem. C* 3, 3211–3218. doi:10.1039/c4tc02685c

- Kuwabara, J., Yasuda, T., Choi, S. J., Lu, W., Yamazaki, K., Kagaya, S., et al. (2014). Direct Arylation Polycondensation: A Promising Method for the Synthesis of Highly Pure, High-Molecular-Weight Conjugated Polymers Needed for Improving the Performance of Organic Photovoltaics. *Adv. Funct. Mater.* 24, 3226–3233. doi:10.1002/adfm.201302851
- Li, W., Guo, Y., Shi, J., Yu, H., and Meng, H. (2016b). Solution-processable Neutral green Electrochromic Polymer Containing Thieno[3,2-B]thiophene Derivative as Unconventional Donor Units. *Macromolecules* 49, 7211–7219. doi:10.1021/acs.macromol.6b01624
- Li, W., and Michinobu, T. (2016). Structural Effects of Dibromocarbazoles on Direct Arylation Polycondensation with 3,4-ethylenedioxythiophene. *Polym. Chem.* 7, 3165–3171. doi:10.1039/c6py00381h
- Li, W., Otsuka, M., Kato, T., Wang, Y., Mori, T., and Michinobu, T. (2016a). 3,6-carbazole vs 2,7-carbazole: A Comparative Study of Hole-Transporting Polymeric Materials for Inorganic-Organic Hybrid Perovskite Solar Cells. *Beilstein J. Org. Chem.* 12, 1401–1409. doi:10.3762/bjoc.12.134
- Liu, D. Y., and Reynolds, J. R. (2010). Dioxythiophene-based Polymer Electrodes for Supercapacitor Modules. *ACS Appl. Mater. Inter.* 2, 3586–3593. doi:10.1021/am1007744
- Meng, Q., Cai, K., Chen, Y., and Chen, L. (2017). Research Progress on Conducting Polymer Based Supercapacitor Electrode Materials. *Nano Energy* 36, 268–285. doi:10.1016/j.nanoen.2017.04.040
- Mercier, L. G., and Leclerc, M. (2013). Direct (Hetero)arylation: A New Tool for Polymer Chemists. *Acc. Chem. Res.* 46, 1597–1605. doi:10.1021/ar3003305
- Murto, P., Elmas, S., Méndez-Romero, U. A., Yin, Y., Genene, Z., Mone, M., et al. (2020). Highly Stable Indacenodithieno[3,2-B]thiophene-Based Donor-Acceptor Copolymers for Hybrid Electrochromic and Energy Storage Applications. *Macromolecules* 53, 11106–11119. doi:10.1021/acs.macromol.0c02212
- Olivier, Y., Niedzialek, D., Lemaire, V., Pisula, W., Müllen, K., Koldemir, U., et al. (2014). 25th Anniversary Article: High-Mobility Hole and Electron Transport Conjugated Polymers: How Structure Defines Function. *Adv. Mater.* 26, 2119–2136. doi:10.1002/adma.201305809
- Österholm, A. M., Ponder, J. F., Jr., Kerszulis, J. A., and Reynolds, J. R. (2016). Solution Processed Pedot Analogues in Electrochemical Supercapacitors. *ACS Appl. Mater. Inter.* 8, 13492–13498. doi:10.1021/acsami.6b02434
- Robitaille, A., Perea, A., Bélanger, D., and Leclerc, M. (2017). Poly(5-alkyl-thieno[3,4-c]pyrrole-4,6-dione): a Study of π -conjugated Redox Polymers as Anode Materials in Lithium-Ion Batteries. *J. Mater. Chem. A* 5, 18088–18094. doi:10.1039/c7ta03786d
- Shown, I., Ganguly, A., Chen, L. C., and Chen, K. H. (2015). Conducting Polymer-based Flexible Supercapacitor. *Energy Sci. Eng.* 3, 2–26. doi:10.1002/ese3.50
- Sun, Y., Zhao, X., Zhu, G., Li, M., Zhang, X., Yang, H., et al. (2020a). Twisted Ladder-like Donor-Acceptor Polymers as Electrode Materials for Flexible Electrochromic Supercapacitors. *Electrochimica Acta* 333, 135495. doi:10.1016/j.electacta.2019.135495
- Sun, Y., Zhu, G., Zhao, X., Kang, W., Li, M., Zhang, X., et al. (2020b). Solution-processable, Hypercrosslinked Polymer via post-crosslinking for Electrochromic Supercapacitor with Outstanding Electrochemical Stability. *Solar Energy Mater. Solar Cell* 215, 110661. doi:10.1016/j.solmat.2020.110661
- Wu, W., Xin, H., Ge, C., and Gao, X. (2017). Application of Direct (Hetero)arylation in Constructing Conjugated Small Molecules and Polymers for Organic Optoelectronic Devices. *Tetrahedron Lett.* 58, 175–184. doi:10.1016/j.tetlet.2016.11.126
- Yamazaki, K., Kuwabara, J., and Kanbara, T. (2013). Detailed Optimization of Polycondensation Reaction via Direct C-H Arylation of Ethylenedioxythiophene. *Macromol. Rapid Commun.* 34, 69–73. doi:10.1002/marc.201200550
- Yigit, D., and Güllü, M. (2018). Capacitive Properties of Novel N-Alkyl Substituted Poly(3,6-Dithienyl-9h-Carbazole)s as Redox Electrode Materials and Their Symmetric Micro-supercapacitor Applications. *Electrochimica Acta* 282, 64–80. doi:10.1016/j.electacta.2018.06.005
- Zhang, H., Li, J., Gu, C., Yao, M., Yang, B., Lu, P., et al. (2016). High Performance, Flexible, Poly(3,4-Ethylenedioxythiophene) Supercapacitors Achieved by Doping Redox Mediators in Organogel Electrolytes. *J. Power Sourc.* 332, 413–419. doi:10.1016/j.jpowsour.2016.09.137

Conflict of Interest: The authors declare that the research was conducted in the absence of any commercial or financial relationships that could be construed as a potential conflict of interest.

Publisher's Note: All claims expressed in this article are solely those of the authors and do not necessarily represent those of their affiliated organizations, or those of the publisher, the editors, and the reviewers. Any product that may be evaluated in this article, or claim that may be made by its manufacturer, is not guaranteed or endorsed by the publisher.

Copyright © 2021 Guo, Zhang, Li, Gong, Wu and Li. This is an open-access article distributed under the terms of the Creative Commons Attribution License (CC BY). The use, distribution or reproduction in other forums is permitted, provided the original author(s) and the copyright owner(s) are credited and that the original publication in this journal is cited, in accordance with accepted academic practice. No use, distribution or reproduction is permitted which does not comply with these terms.